Journal of Solid State Chemistry **143,** 273–276 (1999)
Article ID jssc.1998.8108, available online at http://www.idealibrary.com on IDEAL®

Phase Relations at 1500°C in the Ternary System ZrO_2–Y_2O_3–TiO_2

A. J. Feighery,* J. T. S. Irvine,* D. P. Fagg,*,† and A. Kaiser*

*School of Chemistry, University of St Andrews, St Andrews, Fife, KY16 9ST, Scotland, United Kingdom; and †Department of Chemical Engineering, University of Patras, Patras, Greece

Received July 14, 1998, in revised form November 9, 1998, accepted November 17, 1998

Phase relations at 1500°C in the ternary system ZrO_2–Y_2O_3–TiO_2 have been determined by powder X-ray diffraction of samples prepared by standard solid state mixing and also by ball milling. A large region of this ternary oxide system was shown to exhibit the defect cubic fluorite structure and to encompass compositions containing very high oxygen vacancy concentrations up to 16%, e.g., $Zr_{0.21}Y_{0.62}Ti_{0.17}O_{1.69}$. We have accurately determined the maximum extent of the defect fluorite phase, at low concentrations of yttrium/high concentrations of titanium. From previous studies this region of the solid solution is expected to yield compositions which exhibit the optimum mixed ionic and electronic conducting properties for electrochemical applications. We have determined that at 1500°C up to 18 atom% Ti^{4+} can be dissolved into ZrO_2 stabilized in the cubic fluorite structure by the presence of 14 to 20 atom% Y. Trends in composition and unit cell parameter are discussed. © 1999 Academic Press

INTRODUCTION

Fuel cells offer a means of electrochemical conversion of either hydrocarbon fuels or hydrogen to energy. One of the most promising designs of a fuel cell is the solid oxide fuel cell (SOFC), which is an all-ceramic device that operates at temperatures in the range 850–1000°C (1). This design holds particular promise for power generation, particularly for combined heat and power operation (2).

Most current development centers on designs based on the yttria-stabilized zirconia electrolyte, with Ni/ZrO_2 cermets as the preferred anode (3). The major disadvantages of the Ni cermet anodes are that carbon deposition occurs at the anode (4) and the nickel has low tolerance to sulphur (5). In addition, nickel sinters on prolonged operation (6) and temperature gradients may exist across the anode if both reforming and oxidation occur together.

Our objective has been to address these problems by searching for new anode materials, and attention has been focused on the use of early transition metal oxides. Conducting oxides have several advantages over metals in that they are potentially less likely to promote coking and less likely to suffer from sulphur poisoning. The property of mixed conduction has been suggested to allow electrochemical reactions to occur over the entire electrode–gas interface as opposed to the reaction at solely three point regions between the electrode, electrolyte, and fuel gas in the current cermet materials (7). The potential of titanates for use as SOFC anode materials has been demonstrated in previous work (8, 9), where the accessibility of mixed valence states facilitates electronic conductivity and generally enhances catalytic activity.

In this study, we have investigated the phase relations between ZrO_2, Y_2O_3, and TiO_2 at 1500°C. In particular we have focused on the single phase, defect fluorite region of this ternary system. For these compositions to be considered as SOFC anode materials, the mixed conducting properties must be optimized; i.e., the oxide ion conductivity and the electronic conductivity must be as high as possible in order to have high overall conductivity in the reducing conditions of the fuel gas. Previous work by our research group (10) has shown that the electronic contribution to conductivity is optimized in compositions which contain as much reducible Ti^{4+} as possible. However, in order to dissolve a significant quantity of TiO_2 into ZrO_2, the yttrium/zirconium ratio must be increased beyond that found in 8 mol% YSZ. High levels of the stabilizing dopant Y^{3+} results in high levels of oxygen vacancies and reduced ionic conductivity due to defect interactions (11). Thus, high levels of Y^{3+} lowers the total mixed conductivity.

We have therefore concentrated on the low yttrium, high titanium region of the single phase, defect fluorite region in order to find compositions, which will provide the optimum mixed conducting properties, i.e., maximum Ti^{4+} and minimum Y^{3+}.

EXPERIMENTAL

High purity yttria, zirconia, and titania were used as the starting materials. Samples were ground in acetone using an agate mortar and pestle prior to solid state reaction. For compositions low in Y_2O_3 and high in TiO_2, compositions were prepared by ball milling prior to reaction because the

0022-4596/99 $30.00

more efficient mixing of the reactant oxides was required to obtain phase purity. The powders were uniaxially pressed into pellets (13 mm diameter × 2 mm thick) at a pressure of 2000 kg cm^{-2}. The pellets were presintered at 1000°C for 1 h, heated at 10°C/min to 1500°C, sintered at 1500°C for up to 36 h in air (with intermediate regrinding if required), and then air quenched to room temperature. Densities were measured from pellet geometry and mass. Phase purity was determined using a Philips PW 1830 X-ray diffractometer. Accurate unit cell lattice parameters were determined using a Stoe Stadi-P X-ray diffractometer (10–110° 2θ, Step size 0.02° 2θ, Cu$K\alpha$ radiation) using silicon as an external calibration standard.

RESULTS AND DISCUSSION

In our study we have investigated compositions in the three binary systems, ZrO_2–Y_2O_3(ZY), ZrO_2–TiO_2(ZT), and Y_2O_3–TiO_2(YT), and the ternary system ZrO_2–Y_2O_3–TiO_2(ZYT).

In the ZY binary system, the phase limits are in reasonable accord with the published phase diagram of Scott (12); i.e., the fluorite phase exists between 15 and 57 atom% Y^{3+}. The unit cell increases from 5.1390 Å for 15 atom% Y^{3+} and 5.2447 Å for 57 atom% Y^{3+}. The increase in unit cell size is due to the large Y^{3+} ion dissolving substitutionally into the ZrO_2 structure and introducing oxygen vacancies. Above the 57 atom% Y^{3+} composition, additional lines characteristic of the C-type structure of Y_2O_3 appear in the X-ray powder pattern and splitting of the fluorite peaks is observed. Between 90 and 100 atom% Y^{3+}, only the C-type structure of the Y_2O_3 solid solution is detected. The unit cell parameter of these high Y_2O_3 phases decreases from 10.6040 Å to 10.5652 Å by decreasing the Y^{3+} content from 100 to 90 atom%. The variation in unit cell parameter with composition in the ZY system are shown in Fig. 1.

In the ZT system, a limited solid solution region, with the tetragonal TiO_2 (rutile) structure, was found to exist for 0 to 10 atom% Zr. The $ZrTiO_4$ solid solution, exhibiting an orthorhombic structure, was single phase between 40 and 55 mol% ZrO_2 in agreement with McHale and Roth (13). Thus a two-phase mixture containing $ZrTiO_4$ and TiO_2 (rutile) exists between 10 and 40 atom% ZrO_2. Up to 22 atom% of Ti^{4+} is soluble in tetragonal ZrO_2 at 1500°C. On cooling these samples to room temperature and grinding for X-ray investigation, 100% conversion from tetragonal to monoclinic occurred. The temperature of the monoclinic to tetragonal transition decreases from 1170°C for ZrO_2 to below 1000°C for $Zr_{0.85}Ti_{0.15}O_2$, as determined from DTA studies. On replacing Zr^{4+} with Ti^{4+}, the unit cell size changes from $a = 5.3129$ Å, $b = 5.2125$ Å, $c = 5.1471$ Å, $\beta = 99.218°$ for ZrO_2 to $a = 5.3157$ Å, $b = 5.1403$ Å, $c = 5.1030$ Å, $\beta = 98.908°$ for $Zr_{0.85}Ti_{0.15}O_2$. This decrease in unit cell is in accord with the smaller ionic radius of Ti^{4+} (0.65 Å) compared to that of Zr^{4+} (0.78 Å) (14). No evidence was seen for stabilization of the cubic fluorite structure at 1500°C by Ti^{4+} substitution on its own. The variation in unit cell volume with composition in the ZT system is shown in Fig. 2.

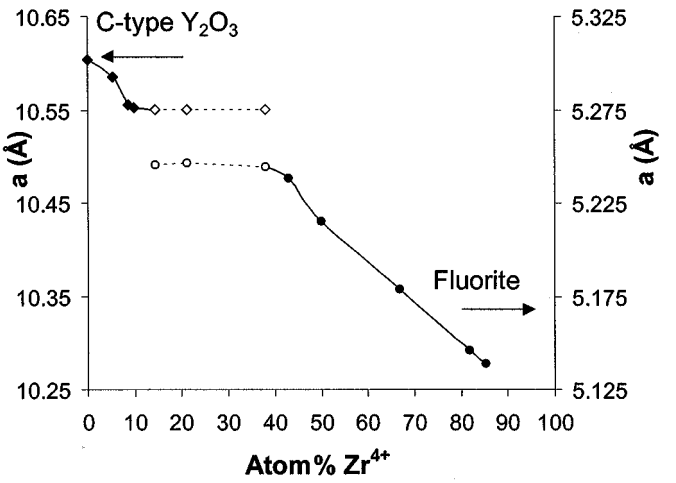

FIG. 1. The binary system ZrO_2–Y_2O_3, the plot of the cubic unit cell parameters for the C-type Y_2O_3 solid solution, and the defect fluorite solid solution vs atom% Zr^{4+}. Note that the C-type unit cell parameter corresponds to double the fluorite unit cell parameter. All data were obtained at 20°C. The open markers reflect a two-phase region.

For the system Y_2O_3–TiO_2 two distinct regions of phase formation were detected. The Y_2TiO_5 line phase is formed at 33.33 atom% Ti^{4+} and a solid solution with the $Y_2Ti_2O_7$ pyrochlore structure exists between 50 and 52 atom% Ti^{4+},

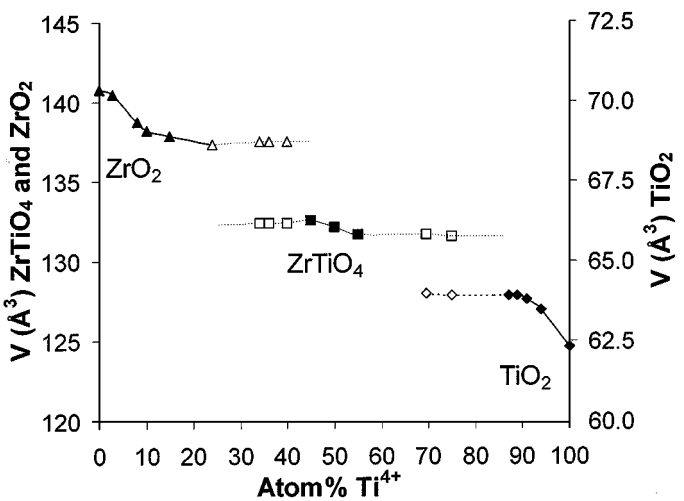

FIG. 2. The binary system TiO_2–ZrO_2, plot of unit cell volume (measured at room temperature) of the tetragonal rutile phase, the monoclinic ZrO_2 solid solution, and the $ZrTiO_4$ solid solution vs atom% Ti^{4+}. Both multiphase regions contain $ZrTiO_4$ solid solution. Note that tetragonal ZrO_2 transforms to monoclinic on cooling. The open markers reflect a two phase region.

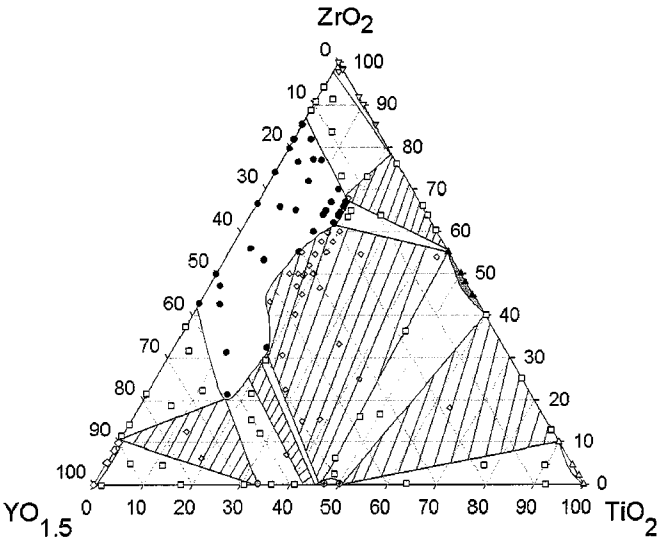

FIG. 3. The experimentally determined phase diagram for the ternary system ZrO_2–Y_2O_3–TiO_2 at 1500°C. ●, cubic fluorite YSZ; ▼, tetragonal ZrO_2; ◆, C-type Y_2O_3; ▲, orthorhombic $ZrTiO_4$; ⊙, pyrochlore $Y_2Ti_2O_7$; ⊜, orthorhombic Y_2TiO_5; ⧋, rutile TiO_2; □, two phase; ◇, three phase.

in agreement with the phase diagram by Mizutani *et al.* (15). The Y_2TiO_5 phase has unit cell parameters $a = 10.333$, $b = 11.181$, and $c = 3.699$ Å. The pyrochlore phase, $Y_2Ti_2O_7$, at 50 atom% Y^{3+} has unit cell parameter $a = 10.0947$ Å.

The ternary phase diagram is shown in Fig. 3. The single phase, two phase, and three phase regions are indicated. No new phases are observed in the ternary system, and apart from the defect fluorite system, none of the binary systems extend significantly into the ternary system. This cubic defect fluorite region extends from the binary ZrO_2–$YO_{1.5}$ join from between 15 and 57 atom% Y^{3+} to almost 20 atom% Ti^{4+} in the ternary system.

A previous study determined that for ZrO_2 stabilized with ~15 atom% Y^{3+}, only 4.5 to 8.5 atom% Ti^{4+} dissolved into the cubic YSZ structure (16). Above this level, peaks attributable to lower symmetry structures of ZrO_2 were detected by X-ray diffraction. Naito and Arashi have reported that for YSZ containing 18 atom% Y^{3+}, specimens containing more than 10.9 atom% Ti^{4+} consisted of two phases (17). Liou and Worrell reported that up to 11–14 atom% Ti^{4+} could be dissolved into YSZ with retention of the cubic fluorite phase (18). Yokokawa *et al.* calculated the maximum solubility of Ti^{4+} in $Zr_{0.85}Y_{0.15}O_{1.925}$ to be 14 atom% at 1573 K (19); this is in good agreement with the experimental value obtained at 1873 K (18).

We have found that for low levels of Y_2O_3 dopant, very little TiO_2 dissolves into the cubic fluorite structure and, e.g., ZrO_2 stabilized with 16.5 atom% Y^{3+} dissolves less than 7 atom% Ti^{4+}. As the amount of Y^{3+} is increased, the solubility of Ti^{4+} increases. With increasing Y^{3+} content, the stabilized cubic fluorite phase can incorporate much more Ti^{4+}. This is probably because the highly defective fluorite structure contains a large number of oxygen vacancies, thus enabling the Ti^{4+} to assume its preferred 6-fold coordination. In stabilized zirconias the oxygen vacancies, which usually associate with Zr^{4+}, also associate with the trivalent dopant cation when it is undersized leading to the formation of MO_6 polyhedra (20).

The maximum extent of this single-phase region in the direction of increasing $YO_{1.5}$ is shown to encompass the composition $Zr_{0.21}Y_{0.62}Ti_{0.17}O_{1.69}$, which has 15.5% of the anion sites vacant. It is surprising that in this direction the defect fluorite region approaches the composition $Y_3TiO_{6.5}$ (a two phase mixture of Y_2O_3 and Y_2TiO_5) instead of the structurally related pyrochlore composition $Y_2Ti_2O_7$. In contrast, in the ternary system Gd_2O_3–TiO_2–ZrO_2 the fluorite and pyrochlore regions coalesce along the $GdO_{1.5}$–ZrO_2 join. Indeed, in the Gd_2O_3 analogue a smooth transition between the pyrochlore and fluorite structures is observed with increasing deviation from $Gd_2M_2O_7$ stoichiometry. This is not surprising as the pyrochlore structure can be viewed as an ordered superstructure of the fluorite structure (21). This obviously shows the significance of the stabilizing dopant size on the resultant structure.

The unit cell parameters in the ternary system were found to increase with Y^{3+} content, as expected from the binary ZY system, and to decrease with increasing Ti^{4+} content. The maximum extent of the fluorite phase in the ternary system for lower levels of aliovalent stabilizing dopant, where the ionic conducting properties are of considerable interest, has been very accurately determined. The maximum limit of the fluorite phase in this low defect region contains compositions with 18 atom% of reducible Ti^{4+}

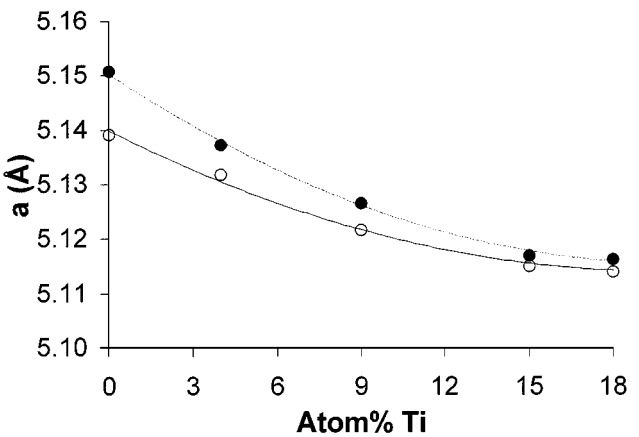

FIG. 4. Comparison of unit cell parameters as a function of Ti^{4+} content for single phase compositions of formula $Zr_{0.85-x}Y_{0.15}Ti_xO_{1.925}$ and $Zr_{0.80-x}Y_{0.20}Ti_xO_{1.9}$ ($0 < x < 0.18$). All data were obtained at 20°C.

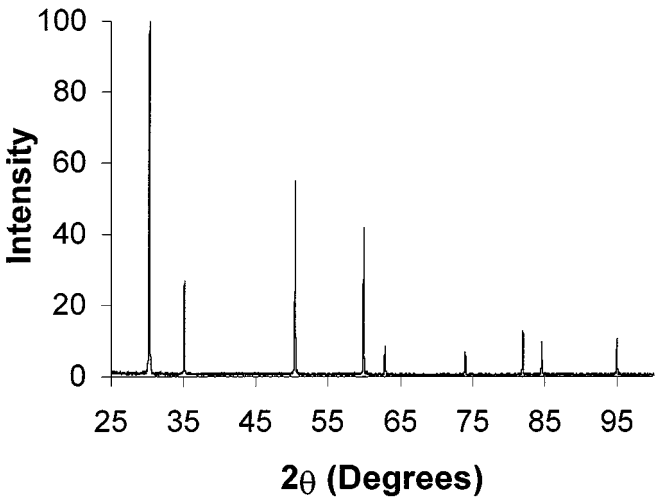

FIG. 5. A typical X-ray diffraction pattern obtained for cubic fluorite materials containing 18 atom% Ti^{4+} stabilized by 14–20 atom% Y^{3+}. (The pattern shown is for $Zr_{0.62}Y_{0.2}Ti_{0.18}O_{1.90}$).

and with between 14 and 20 atom% of stabilizing Y^{3+}, i.e., compositions with formula $Zr_{1-x}Y_xTi_{0.18}O_{2-(x/2)}$ for $0.14 \leq x \leq 0.20$.

Figure 4 shows the variation in unit cell parameter with composition for single phase cubic fluorite compositions. The X-ray diffraction pattern for the titanium rich composition $Zr_{0.62}Y_{0.20}Ti_{0.18}O_{1.9}$ is shown in Fig. 5 with the peak data listed in Table 1.

CONCLUSIONS

A large defect fluorite solid solution exists in the ternary ZrO_2–Y_2O_3–TiO_2 system. The amount of TiO_2 which dissolves into ZrO_2 is highly dependent upon the quantity of stabilizing aliovalent dopant. The aliovalent dopant introduces oxygen vacancies into the fluorite lattice, thus enabling the smaller Ti^{4+} ion to assume a 6-fold coordination environment. A maximum of 18 atom% Ti^{4+} can be dissolved into YSZ stabilized in the fluorite structure by 14–20 atom% Y^{3+}, with oxygen vacancy concentrations of 2.9 and 6.25%, respectively. Further studies are underway to determine if the electrochemical properties of this system are suitable for use as solid oxide fuel cell materials and to determine if there are any aging effects in the fuel cell operating temperature range of 850–1000°C.

TABLE 1
Refined Peak Data Obtained for $Zr_{0.62}Y_{0.20}Ti_{0.18}O_{1.90}$ at 20°C

2θ	d	hkl	Intensity
30.238	2.9532	111	100
35.057	2.5575	200	26.3
50.404	1.8090	220	54.5
59.913	1.5426	311	41.8
62.871	1.4769	222	8.2
74.049	1.2792	400	6.7
82.014	1.1739	331	13.2
84.625	1.1443	420	9.0
95.040	1.0444	422	10.6

ACKNOWLEDGMENTS

We thank the EPSRC and Tioxide Specialities, Ltd. for financial support and the Nuffield Foundation for a Science Research Fellowship.

REFERENCES

1. B. C. H. Steele, *Mat. Res. Bull.* **14,** 19 (1989).
2. D. S. Beison and M.R. Taylor, UK Department of Industry Report ETSU/FCR/008.
3. N. H. Minh, *J. Am. Ceram. Soc.* **76,** 563 (1993).
4. B. C. H. Steele, I. Kelly, H. Middleton, and R. Rudkin, *Solid State Ionics* **28–30,** 1547 (1988).
5. N. S. Jacobson and W. L. Worrell, *Proc. High Temp. Mater.* **2,** 217 (1983).
6. F. P. F. van Berkel, F. H. van Heuveln, and J. P. P Huijsmans, *Solid State Ionics* **72,** 636 (1993).
7. M. Mogensen, *in* "Proc. 14th Int. Mater. Sci." (F. W. Poulsen, J. J. Bentzen, T. Jacobsen, E. Skou, and M. J. L. Ostergard, Eds.). High Temp. Electrochem., Behaviour Fast Ion and Mixed Cond., p. 117. Risø Nat. Lab., Denmark, 1993.
8. D. P. Fagg, S. M. Fray, and J. T. S. Irvine, *Solid State Ionics* **72,** 235 (1994).
9. H. J. Steiner, P. H. Middleton, and B. C. H. Steele, *J. Alloys and Compounds* **190,** 279 (1993).
10. D. P. Fagg, PhD Thesis, University of Aberdeen, 1996.
11. D. K. Honke, *Solid State Ionics* **5,** 531 (1981).
12. H. G. Scott, *J. Mat. Sci.* **10,** 1527 (1975).
13. A. E. McHale and R. S. Roth, *J. Am. Ceram. Soc.* **66,** C18–C20 (1983).
14. R. D. Shannon, *Acta Crystallogr. A* **32,** 751 (1976).
15. N. Mizutani, Y. Tajima, and M. Kato, *J. Am. Ceram. Soc.* **59,** 168 (1976).
16. L. S. M. Traqueia, T. Pagnier, and F. M. B. Marques, *J. Eur. Ceram. Soc.* **17,** 1019 (1997).
17. H. Arashi and H. Naito, *Solid State Ionics* **53–56,** 431 (1992).
18. S. S. Liou and W. L. Worrell, *Appl. Phys. A* **49,** 25 (1989).
19. H. Yokokawa, T. Horita, N. Sakai, M. Dokiya, J. Van Herle, and S. G. Kim, *Denki Kagaku* **64,** No. 6, 690–691 (1996).
20. Ping. Li and I-Wei Chen, *J. Am. Ceram. Soc.* **77,** No. 1, 118–128 (1994).
21. A. J. Feighery, J. T. S. Irvine, and C. Zheng, *Ionics* **3,** 30 (1997).